

Effect of Interfacial Shear and Entrainment Models on Flooding Predictions

N. K. Popov and U. S. Rohatgi

Department of Nuclear Energy
Brookhaven National Laboratory
Upton, NY 11973

Introduction

The countercurrent annular flow in vertical pipes and its limitation, namely flooding, is important for the operation of emergency core cooling systems in LWR nuclear plants, as well as in other physical situations.

In this paper an analysis has been developed for adiabatic, steady-state, one-dimensional, air-water flow to predict flooding phenomenon. The formulation consists of separated flow analysis of the film and gas-droplet mixture in the pipe. The droplet phase of the pipe core is treated with a drift-flux model. Many correlations for interfacial shear, entrainment, inception, and rate available in the literature have been used in this analysis. Furthermore, recent versions of TRAC-PF1 and RELAP5/MOD1, along with the present analysis, have been applied to model the University of Houston countercurrent flow tests. The effects of various constitutive relationships have been compared. Some suggestions for model improvement have also been given.

Countercurrent flow situations arise in downcomers, or spray systems of nuclear reactors, etc., during emergency cooling operation. This phenomenon is of major concern and has been modeled as an interaction of falling film and upward flowing gas by many investigators. In particular, great efforts have been made to understand the conditions that lead to transition to cocurrent upward flow. Among many parameters which influence the flooding phenomenon, only interfacial shear stress, entrainment inception, and rate have been investigated here.

Generally, there are two ways to predict flooding or countercurrent flow limitation. In the first approach, a correlation based on data on limit of countercurrent flow is used; in the second approach an analysis of flow is performed using conservation equations and constitutive relationships. The examples of the first approach are the Wallis (1969, 1970a,b) and Kutateladze (1972) correlations:

$$j_g^{*1/2} + m j_f^{*1/2} = C_1 \quad (1)$$

During the work reported here, N. K. Popov was visiting scientist from the University Kiril and Metodij-Skopje, Yugoslavia.

$$K_g^{1/2} + n K_f^{1/2} = C_2 \quad (2)$$

where

$$j_i^* = \rho_i^{1/2} j_i [g d (\rho_f - \rho_g)]^{-1/2} \quad (3)$$

$$K_i = \rho_i^{1/2} j_i [g \sigma (\rho_f - \rho_g)]^{-1/4} \quad (4)$$

Many other investigators (Chung et al., 1980; Imura et al., 1977; Tien et al., 1980) have modified coefficients in Eqs. 1 and 2 to account for other effects such as geometry or condensation.

In this paper, a second approach is used to predict the University of Houston countercurrent flow tests (Dukler and Smith, 1979; Dukler, 1980). This approach provides a means of comparing the effectiveness of various constitutive relationships such as interfacial shear, entrainment inception, and rate in predicting countercurrent flow.

Most of the constitutive relationships needed for this analysis have been developed from cocurrent flow data and some are also used in advanced codes such as RELAP5 (Ransom, 1982) and TRAC-PF1 (Liles, 1981).

There are many definitions of flooding, such as the inception of droplets, liquid film flow reversal, no downward film flow, formation of liquid bridge, or sudden increase in pressure gradient across the test section. Most of these conditions occur at similar gas flow rates. In the present analysis, a sudden increase in the film thicknesses of bridging of the test section is used as an indication of flooding.

Modeling

Formulation of the Problem and Assumptions

The physical system analyzed here consisted of a vertical pipe with a liquid film flowing downward at the wall. The core of the pipe was occupied by the upward flowing mixture of the gas and entrained liquid droplets. The liquid and the gas mass flow rates entering the pipe were assumed to be constant. Any heat transfer from the pipe was neglected. Also, due to relatively low pressure gradients in the pipe, liquid and gas thermohydraulic

properties were assumed to be constant. The details of the formulation have been given by Popov and Rohatgi (1985).

For the purpose of comparison of the models for interfacial shear and the entrainment models with the data (Dukler and Smith, 1979), a one-dimensional analysis was chosen. Many investigators have reported the effect of liquid film velocity profile on interfacial velocity and flooding (Hewitt, 1963) or even the possibility of the existence of some downflow and some upflow of the film at the same time (Maron and Dukler, 1981). However, consistent with one-dimensional analysis, it was assumed that the liquid film and the gas core have uniform velocities. The gas-liquid interface velocity had been taken as the average liquid film velocity. It had been suggested that interfacial waves play a major role in the flooding phenomena (Shearer and Davidson, 1965; Chu and Dukler, 1975; Tien et al., 1980). However, in the present analysis, their influence had been accounted for through constitutive equations. Furthermore, inception of bridging or rapid increase in the film thickness was assumed as a flooding criterion. The liquid and gas phases were modeled with a two-fluid approach. The core fluid was treated as a mixture of droplets and air which interacted with the film at the interface. This led to the following definitions:

$$\alpha_c + \alpha_f = 1 \quad (5)$$

$$\bar{\alpha}_d + \bar{\alpha}_g = 1 \quad (6)$$

where α_c , α_f , $\bar{\alpha}_d$, and $\bar{\alpha}_g$ are fractions of pipe area occupied by the core and the film, and fractions of the core area occupied by the droplets and the air, respectively.

Balance Equations

As the film and air flow phenomena modeled here are adiabatic in nature, only mass and momentum balances are needed. The film and core are treated with a two-fluid approach and the droplets in the core are modeled with a drift-flux formulation. The three mass balances for core mixture, droplets and liquid film are as follows (Popov and Rohatgi, 1985):

$$-A\rho_c V_c \frac{d\alpha_f}{dx} + (\rho_d - \rho_g)(1 - \alpha_f)AV_c \frac{d\bar{\alpha}_d}{dx} + (1 - \alpha_f)A\rho_c \frac{dV_c}{dx} = -S'_d \quad (7)$$

$$-A\rho_d \bar{\alpha}_d \left[V_c - \frac{\rho_g}{\rho_c} V_{dj} \right] \frac{d\alpha_f}{dx} + A\rho_d (1 - \alpha_f) \{ V_c - \rho_g V_{dj} (\rho_c + \rho_g) / \rho_c^2 \} \frac{d\bar{\alpha}_d}{dx} + A\rho_d (1 - \alpha_f) \alpha_d (1 + 0.9\rho_g V_{dj} / \rho_c V_c) dV_c / dx = -S'_d \quad (8)$$

$$\left(\rho_f V_f \frac{d\alpha_f}{dx} + \rho_f \alpha_f \frac{dV_f}{dx} \right) A = -S'_d \quad (9)$$

where S'_d , V_{dj} , V_c , and ρ_c are net droplet entrainment per unit length, droplet drift velocity, core mixture velocity, and density, respectively. The core velocity and density are defined as:

$$\rho_c = \bar{\alpha}_d \rho_d + (1 - \bar{\alpha}_d) \rho_g \quad (10)$$

$$V_c = [\rho_d \bar{\alpha}_d V_d + (1 - \bar{\alpha}_d) \rho_g V_g] / \rho_c \quad (11)$$

The droplet drift velocity is obtained from Ishii's (1977) correlation:

$$V_{dj} = 1/2 \bar{\alpha}_d r_d [(g\Delta\rho)^2 / \mu_g \rho_g]^{1/3} \quad (12)$$

where the droplet radius r_d is given by Tatterson et al. (1977) as:

$$r_d = 0.0112 \frac{d^{0.6} \sigma^{0.5}}{\mu^{0.1} \rho_g^{0.4}} V_g^{-0.9} \quad (13)$$

Besides the mass balance, the analysis also needs momentum balance for the pipe core and the film. These two balance equations, after some manipulation, are (Popov and Rohatgi, 1985):

$$A(1 - \alpha_f) \frac{dp}{dx} - A \frac{\rho_d \rho_g \bar{\alpha}_d}{(1 - \bar{\alpha}_d)} \frac{V_{dj}^2}{\rho_c} \frac{d\alpha_f}{dx} + A \frac{(1 - \alpha_f)}{(1 - \bar{\alpha}_d)} \frac{\rho_d \rho_g}{\rho_c} V_{dj}^2 \left[\frac{1}{(1 - \bar{\alpha}_d)} + 2 - \bar{\alpha}_d \frac{(\rho_d - \rho_g)}{\rho_c} \right] \frac{d\bar{\alpha}_d}{dx} + A(1 - \alpha_f) \left[\rho_c V_c - 1.8 \frac{\rho_d \rho_g \bar{\alpha}_d}{(1 - \bar{\alpha}_d) \rho_c} \frac{V_{dj}^2}{V_c} \right] \frac{dV_c}{dx} = A(1 - \alpha) \rho_f g_c + \tau'_{w,f} + S'_d (V_c + V_f) \quad (14)$$

$$A\alpha_f \frac{dp}{dx} + A\alpha_f \rho_f V_f \frac{dV_f}{dx} = A\alpha_f \rho_f g - \tau'_{w,f} - \tau'_{i,f} \quad (15)$$

where $\tau'_{w,f}$ and $\tau'_{i,f}$ are wall and interfacial shear stresses. These five equations along with constitutive relations completely describe the problem. This system of equations is solved by the Adams-Moulton predictor-corrector method from the liquid entrance at the top to the air entrance at the bottom of the test section.

Constitutive Equations

Wall shear stress

The liquid film wall shear stress is expressed as:

$$\tau'_{w,f} = \tau''_{w,f} P_w = 1/2 f_w \rho_f V_f^2 P_w \quad (16)$$

Since there is no major difference between the wall friction coefficients for film and full pipe flow (Ishii et al., 1976), it is given as (Thurgood et al., 1981):

$$f_w = 16/Re_f \quad Re_f \leq 1,000 \quad (17)$$

$$f_w = 0.0791 Re^{-0.25} \quad Re_f > 1,000 \quad (18)$$

where the liquid film Reynolds number is defined (Ishii et al., 1976) as:

$$Re_f = \frac{\rho_f j_f d}{\mu_f} \approx \frac{4\delta \rho_f V_f}{\mu_f} \quad (19)$$

Interfacial shear stress

The interfacial shear stress is defined as:

$$\tau'_{i,f} = \tau''_{i,f} P_I = [0.5 f_I \rho_c (V_c + V_f)^2] [\pi d \sqrt{1 - \alpha_f}] \quad (20)$$

In this equation the effect of entrained droplets moving in the gas stream on the shear stress has been taken into account by using the core mixture properties.

The following five correlations for the interfacial friction coefficients have been compared:

1. Wallis Correlation (Wallis, 1969)

$$f_I = 0.005[1 + 300 \delta/d] \quad (21)$$

2. OBRA-TF Correlations (Thurgood, 1981)

Equation 21 is also used here for the stable and smooth films. However, when the film thickness exceeds a critical film thickness as described here, the film is considered unstable.

$$(\alpha_f)_{\text{crit}} = \frac{4C_s \sigma}{\rho_g d (V_c + V_f)^2} \quad (22)$$

$$C_s = 0.5 \quad (23)$$

For unstable and very wavy films, the interfacial friction coefficient is (Thurgood, 1981; Henstock and Hanratty, 1976):

$$f_I = \max \left\{ f_s \left[1 + 1,400 F \left\{ 1 - \exp \left(\frac{1}{G} \frac{(1 + 1,400 F)^{3/2}}{13.2} \right) \right\} \right] \right. \quad (24)$$

$$\left. 0.025[1 + 150(1 - \sqrt{1 + \alpha_f})] \right\} \quad (25)$$

where f_s can be estimated from the expression in Eq. 18 and other variables are:

$$G = \frac{\rho_f g d}{\rho_g V_g^2 f_s} \quad (26)$$

$$F = \frac{m^+ \mu_f}{Re_g^{0.9} \mu_g} \sqrt{\rho_g / \rho_f} \quad (27)$$

$$m^+ = [(0.707 Re_f^{0.5})^{2.5} + (0.0379 Re_f^{0.9})^{2.5}]^{0.4} \quad (28)$$

3. Bharathan-Wallis Correlation (Bharathan et al., 1979)

This correlation accounts for the surface tension effect and is given as:

$$f_I = 0.005 + C_{f1} \delta^* C_{f2} \quad (29)$$

where

$$C_{f1} = 0.275 \cdot 10^{9.07} / d^* \quad (30)$$

$$C_{f2} = 1.63 + 4.74 / d^* \quad (31)$$

and the dimensionless film thickness and diameter are defined as:

$$\delta^* = \delta / \sqrt{\sigma / (g(\rho_f - \rho_g))} \quad (32)$$

$$d^* = d / \sqrt{\sigma / (g(\rho_f - \rho_g))} \quad (33)$$

4. Dukler's Correlation (Dukler, 1980)

The countercurrent part of this correlation is shown in Figure 1 and is also described here as:

$$f_I = \left[3.04 \log \left(\frac{d}{\delta} Re_g \right) - 16.16 \right]^{-2} \quad (34)$$

with

$$Re_g = \frac{d \sqrt{1 - \alpha_f} \rho_g V_g}{\mu_g} \quad (35)$$

A slightly modified version of this correlation has been used in TRAC-PF1 (Liles et al., 1981).

5. Modified Wallis Correlation

The original Wallis (1969) correlation is used until the inception of entrainment, thereafter a modified Wallis correlation is suggested to account for increased roughness. This correlation is shown in Figure 2 and is:

$$f_I = [0.005 + 1.5 \delta/d][V_r/(V_r)_{\text{crit}}]^{2.5} \quad (36)$$

This modification is based on University of Houston data (Dukler and Smith, 1979), and $v_{r,\text{crit}}$ is described as

$$v_{r,\text{crit}} = \frac{2.6\sigma}{\mu_f} \sqrt{\frac{\rho_f}{\rho_g}} N_\mu^{0.8} Re_f^{-0.2} \quad (37)$$

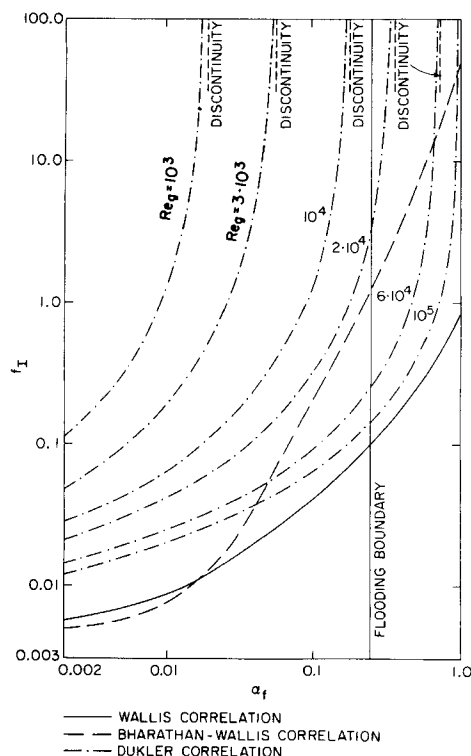


Figure 1. Interfacial friction coefficient.

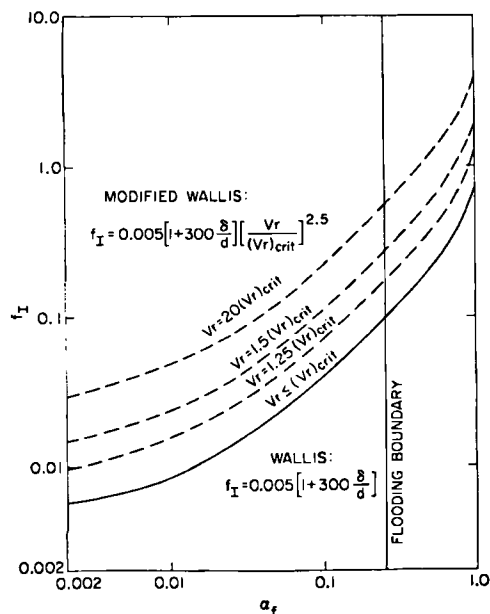


Figure 2. Interfacial friction coefficient.

where the viscosity number is defined as:

$$N_\mu = \mu_f \left(\rho_f \sigma \sqrt{\frac{\sigma}{g(\rho_f - \rho_g)}} \right)^{-1/2} \quad (38)$$

Entrainment

The balance equations also need a correlation for net droplet entrainment S'_d :

$$S'_d = EW_f/H \quad (39)$$

Five of the correlations from the literature and their modified forms for entrainment rate E have been used here in the analysis and are listed as follows:

1. COBRA-TF Entrainment Inception and Rate Model

The entrainment model in COBRA-TF is based on a critical film thickness concept as described here:

$$E = [\alpha_f - (\alpha_f)_{crit}] \rho_f V_f A \quad (40)$$

where $(\alpha_f)_{crit}$ has been described in Eq. 22.

This model implies that all the fluid in the film in excess of critical film thickness $(\alpha_f)_{crit}$ will be entrained.

2. Ishii's Correlations for Entrainment Inception and Rate

Ishii and Grolmes (1975) and Ishii and Mishima (1981) developed correlations for entrainment inception and rate from cocurrent data.

The entrainment inception criterion in this correlation for laminar flow is:

$$V_{r,crit} = 11.78 \frac{\sigma}{\mu_v} \sqrt{\frac{\rho_f}{\rho_g}} N_\mu^{0.8} Re_f^{-1/3} \quad \begin{matrix} 2 < Re_f < 1635 \\ N_\mu \leq 1/15 \end{matrix} \quad (41)$$

and for turbulent flow it is:

$$V_{r,crit} = \frac{\sigma}{\mu_f} \sqrt{\frac{\rho_f}{\rho_g}} N_\mu^{0.8} \quad \begin{matrix} Re_f \geq 1635 \\ N_\mu \leq 1/15 \end{matrix} \quad (42)$$

where the viscosity number has been defined in Eq. 38. Equilibrium entrainment (Ishii and Mishima, 1981) is achieved in an

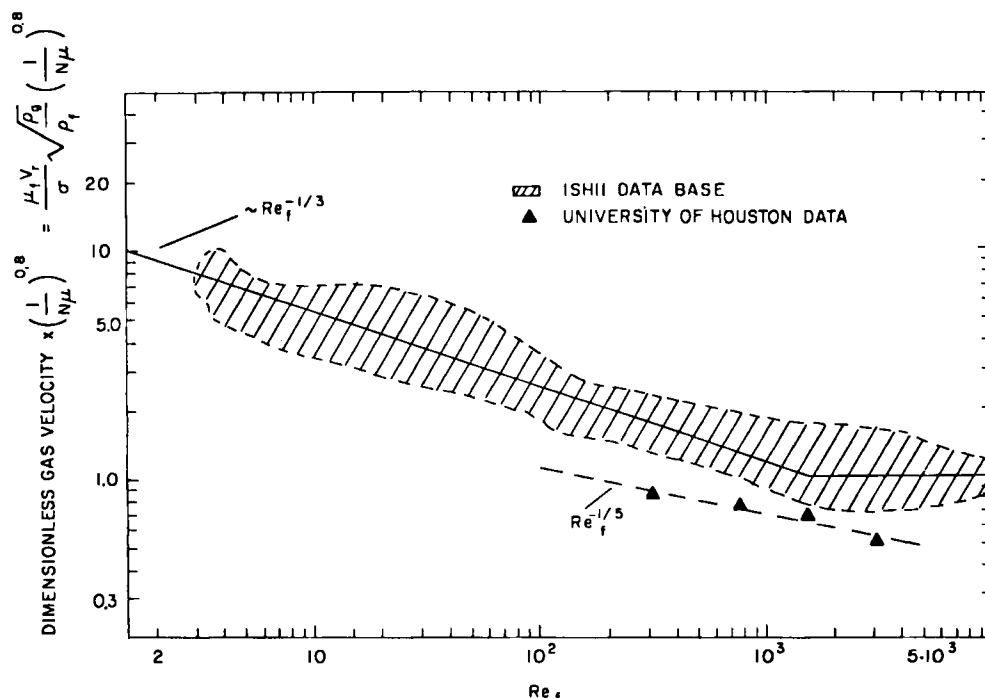


Figure 3. Entrainment inception criterion.

axial length defined as:

$$L_{eq} = 600 d \sqrt{\frac{V_r^*}{Re_f}} \quad (43)$$

where the dimensionless relative velocity is given by:

$$V_r^* = (V_c + V_f) \left[\frac{\sigma g (\rho_f - \rho_g)}{\rho_g^2} \left(\frac{\rho_g}{\rho_f - \rho_g} \right)^{2/3} \right]^{-1/4} \quad (44)$$

The entrainment rate is given by:

$$E = E_{eq} [1 - \exp(-10^{-5} \psi^2)] \quad (45)$$

Where ψ and E_{eq} are the relaxation function and equilibrium entrainment rate respectively, and are defined as:

$$\psi = \frac{x}{d} \sqrt{Re_f / V_r^*} \quad (46)$$

$$E_{eq} = \tanh(7.25 \cdot 10^{-7} V_r^{*2.5} d^{*1.25} Re_f^{0.25}) \quad (47)$$

3. Ishii Entrainment Correlation with Modified Inception

In the first attempt at improving the models for countercurrent entrainment, the inception criterion given by Ishii in Eq. 41 was tested with the data.

This criterion was developed from a cocurrent data base and is not very accurate for countercurrent flows. It was modified to have better agreement with the countercurrent data as shown in Figure 3, and is given here:

$$V_{r,crit} = \frac{2.6\sigma}{\mu_f} \sqrt{\frac{\rho_f}{\rho_g} N_\mu^{0.8} Re_f^{-0.2}} \quad (48)$$

The entrainment rate was obtained from Ishii's original model as given by Eqs. 45 and 47.

4. Modified Ishii Entrainment Correlations

Ishii's original entrainment correlation was developed from cocurrent data and so it was modified to have a better match with countercurrent data. Figure 4 shows a comparison of the original and modified correlations with the data (Dukler and Smith, 1979). The modified correlation is:

$$E = \tanh(2.9 \cdot 10^{-6} V_r^{*2.5} d^{*1.25} Re_f^{0.25}) \quad (49)$$

As there is a great deal of uncertainty with the entrance effect, Eq. 49 was used throughout the flow field. Furthermore, the inception criterion used is the same as given by Eq. 48.

5. TRAC-PF1 Entrainment Model

TRAC-PF1 (Liles et al., 1981) has an entrainment model based on the critical gas velocity. The entrainment inception takes place when the gas velocity is greater than $V_{g,crit}$. The model is as follows:

$$V_{g,crit} = 2.3[(\rho_g - \rho_f)\sigma We_d / \rho_g^2]^{0.25} \quad (50)$$

$$E = 1 - \exp[-(V_g - V_{g,crit})0.23]$$

No data base was provided for this model in the reference.

University of Houston Test Description

The test section was a 4.11 m long, 0.05 m I.D. vertical tube. The water at ambient pressure and temperature were injected in the middle of the test section through a 0.225 m long porous sec-

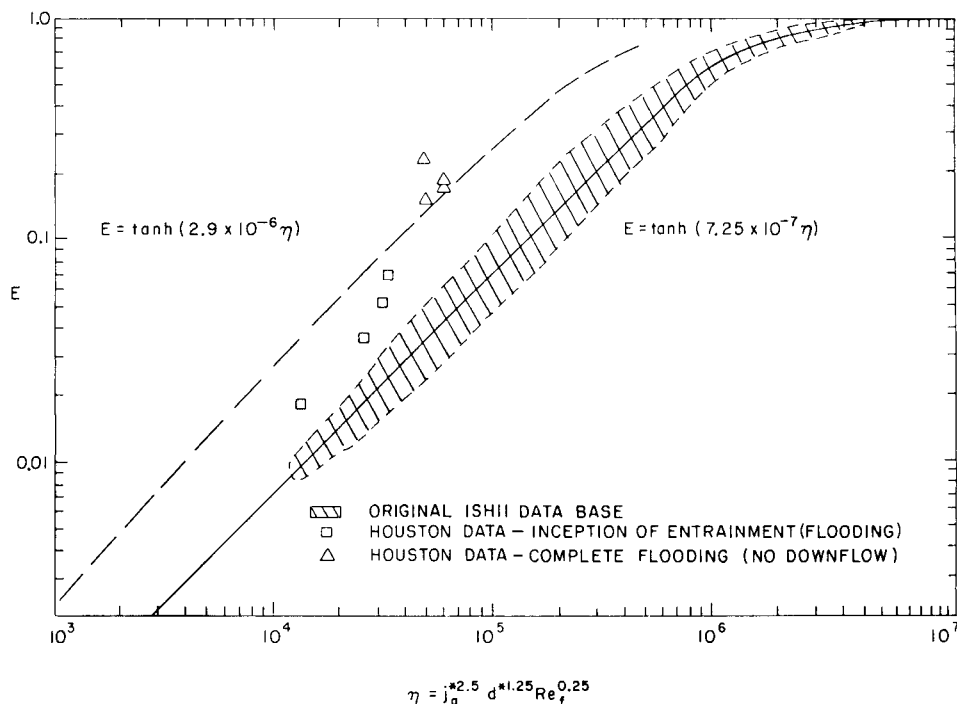


Figure 4. Entrainment rate.

Table 1. Identification Data for Figures 5-8

| Interfacial Shear | Entrainment | Symbol | Equation |
|--|----------------------------|--------|----------|
| Wallis | None | + | 21 |
| Wallis | Ishii correlation | ○ | 21 |
| | modified | | 47 |
| | inception | | 48 |
| Wallis | Modified Ishii correlation | ▽ | 21 |
| | | | 48 |
| | | | 49 |
| COBRA-TF | COBRA-TF | □ | 22, 36 |
| | | | 27 |
| Bharathan-Wallis | Modified Ishii correlation | * | 48 |
| | | | 49 |
| Modified Wallis | None | ⊕ | 36 |
| | | | 36 |
| Modified Wallis | Modified Ishii correlation | ⊕ | 48 |
| | | | 49 |
| Trac-PFI Runs | | ■ | 35, 50 |
| Houston experiment—Entrainment inception | | ▼ | — |
| Houston experiment—Film upflow inception | | ● | — |

tion surrounded by a jacket. The air at ambient pressure and temperature was supplied at the bottom through a collecting chamber. This chamber was also used to collect and measure the water downflow rate. The top of the test section was connected to another chamber in which the liquid film was separated from the air-droplet mixture and the upward film flow rate was mea-

sured. The air-droplet mixture was passed through a separator and the entrained liquid flow rate was measured. There were four stations on the test section for film thickness measurements and four more stations for pressure measurements. Further details of the test section and instrumentation can be found in the data report by Dukler and Smith (1979).

Four different water feed rates were used: 0.0126, 0.0315, 0.063, and 0.126 kg/s. In each series of tests the airflow rate was gradually increased from 0.01512 to 0.0378 kg/s. The air flow rate at the flooding point or the onset of liquid upflow increased as the water feed flow rate was decreased. The water feed rates of 0.0126 and 0.126 kg/s produced two distinctly different flooding situations. Furthermore, this data report identified the flooding point as the air flow rate at which the entrainment began. However, this air flow rate was different from the air flow rate at which the film reversed.

Results and Discussion

Many combinations of constitutive relationships have been used to predict the flow between the liquid entrance and the air entrance. Some of these constitutive relationships have been compared in Figures 1 through 4. Figure 1 shows a comparison of the Wallis, Bharathan-Wallis, and Dukler correlations for the interfacial shear coefficient. Dukler's correlation has a dependence on the gas Reynolds number and is used in TRAC-PFI. The Wallis and the Bharathan-Wallis correlations predict the same coefficient for the thin film, but the latter correlation computes a much higher coefficient for thicker films. A modified

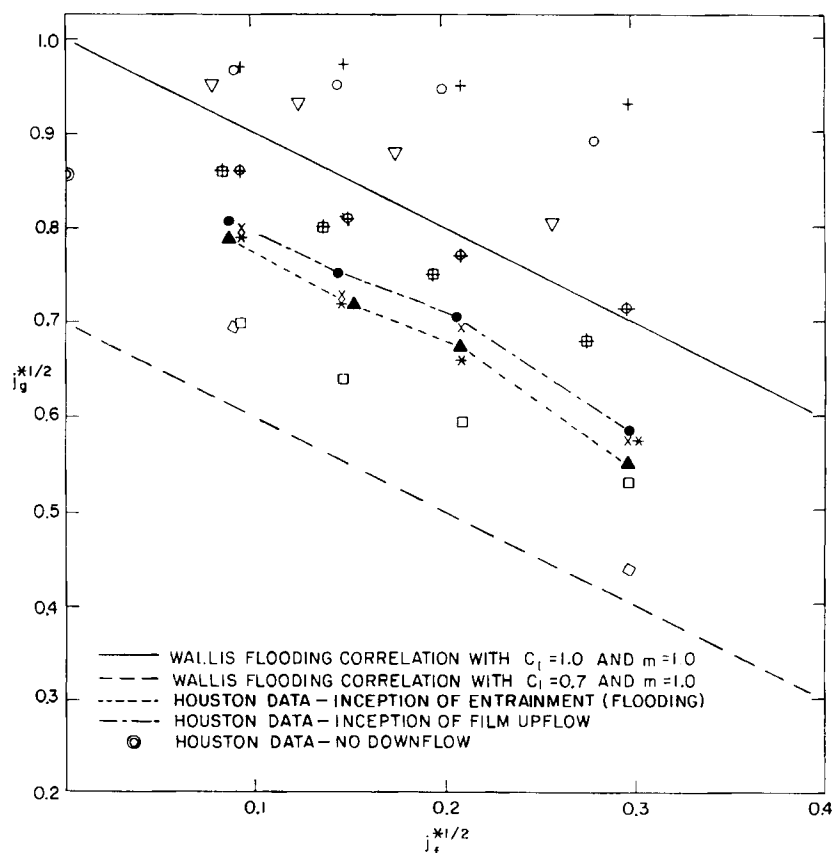


Figure 5. Flooding prediction.

Wallis correlation for the interfacial shear coefficient has been suggested, and this correlation accounts for the increase in roughness with increase in gas velocity after the inception of entrainment. This correlation is shown in Figure 2. It will be shown later that this modified Wallis correlation does a better job than the other two. Besides the interfacial shear, the other constitutive relations used are entrainment inception and rate. They are shown in Figures 3 and 4. Among many correlations, the correlation of Ishii and Mishima (1981) has the widest data base and has been chosen here. It should be noted that most of the data base is cocurrent flow. Figure 3 shows that the correlation due to Ishii and Mishima predicts much later inception than the Houston test data indicates, and that a function of $Re_f^{1/5}$ will correlate the data better. Ishii's original inception criterion has not been used in any of the calculations. Figure 4 shows that Ishii's (1981) correlation predicts lower entrainment rate than the test data. In reality the difference should be more, as the test data are at the exit of the test section and some of the droplets may have deposited on the dry tube above the liquid injection region. Based on this, a modified Ishii inception criterion and rate have been proposed and are shown in Figures 3 and 4.

The next set of figures shows the comparison of various countercurrent flow limits predicted by the analysis for different constitutive relationships. Table 1 gives the notations for each combination as used in Figures 5 to 8.

Figures 5 and 6 show the limit of countercurrent flow for vari-

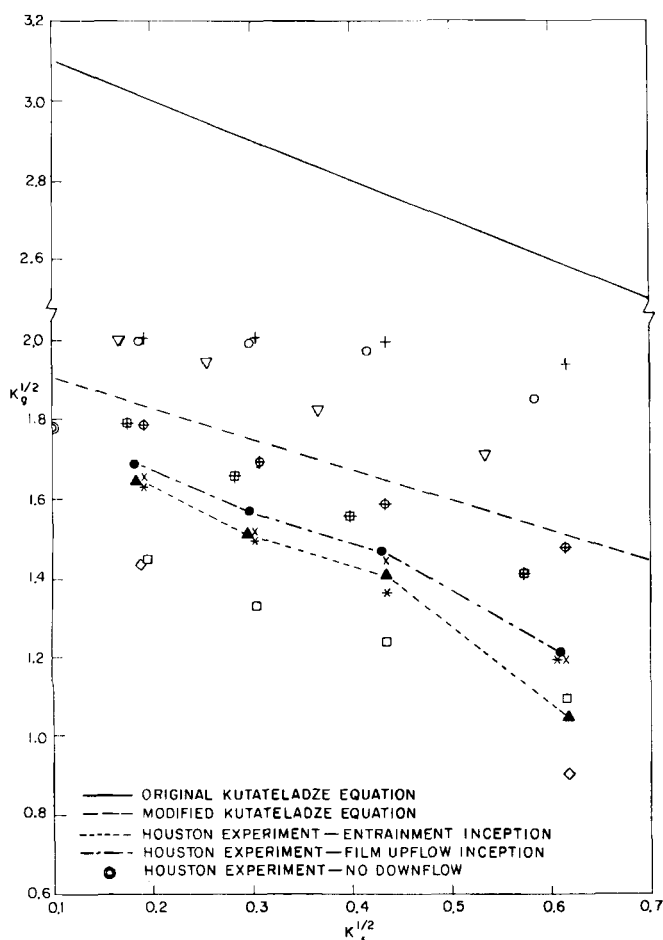


Figure 6. Flooding prediction.

ous combinations of constitutive relations. For this University of Houston test, the Wallis flooding curves bound the data while the original and modified Kutateladze curves (Chung et al., 1981) are above the data. Furthermore, there is a large spread in predictions. TRAC-PF1 computed the lowest value of gas flow rate, while a combination of Wallis interfacial shear model and no entrainment predicted the highest value of gas flow rate required to support a given liquid downflow. The Bharathan-Wallis correlation for interfacial shear along with the modified Ishii entrainment model produced the best agreement with the data.

Besides a countercurrent flow limit, there are other aspects of flow such as film thickness, pressure gradient, etc., which should also be compared. Figure 7 shows the comparison between the predicted and measured film thicknesses at the bottom of the test section for various liquid injection rates. The data showed a sudden increase in film thicknesses at the flooding point in the test section. Among three approaches considered, the Bharathan-Wallis and the modified Wallis correlation for interfacial shear had better agreement. The Wallis correlation computed the lowest interfacial shear and thinnest film at higher gas flow rates. Figure 8 shows the pressure gradient in the test section for various liquid injection rates. At the flooding point, the pressure gradient increases. The Bharathan-Wallis correlation overpredicted the pressure gradient by a large margin, while the modified Wallis correlation showed a much better agreement. Both these computations used the modified Ishii entrainment correlation. Based on these comparisons, the modified Wallis correlation, and the modified Ishii entrainment model should be given further consideration.

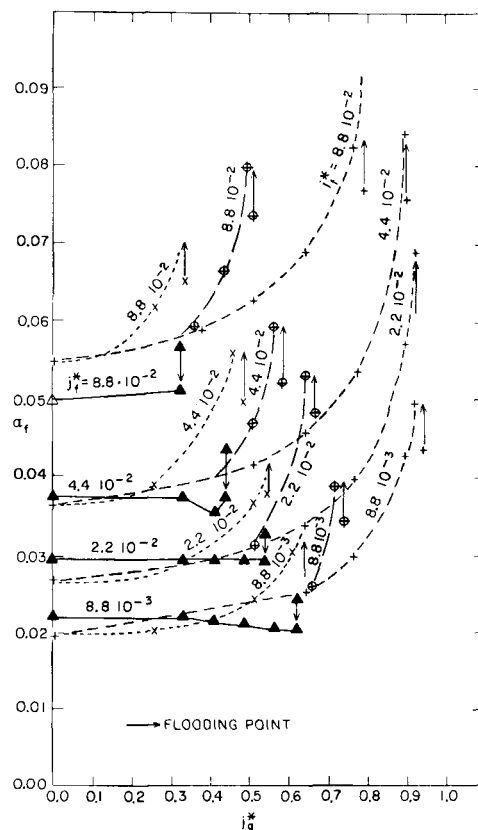


Figure 7. Film volume fraction prediction.

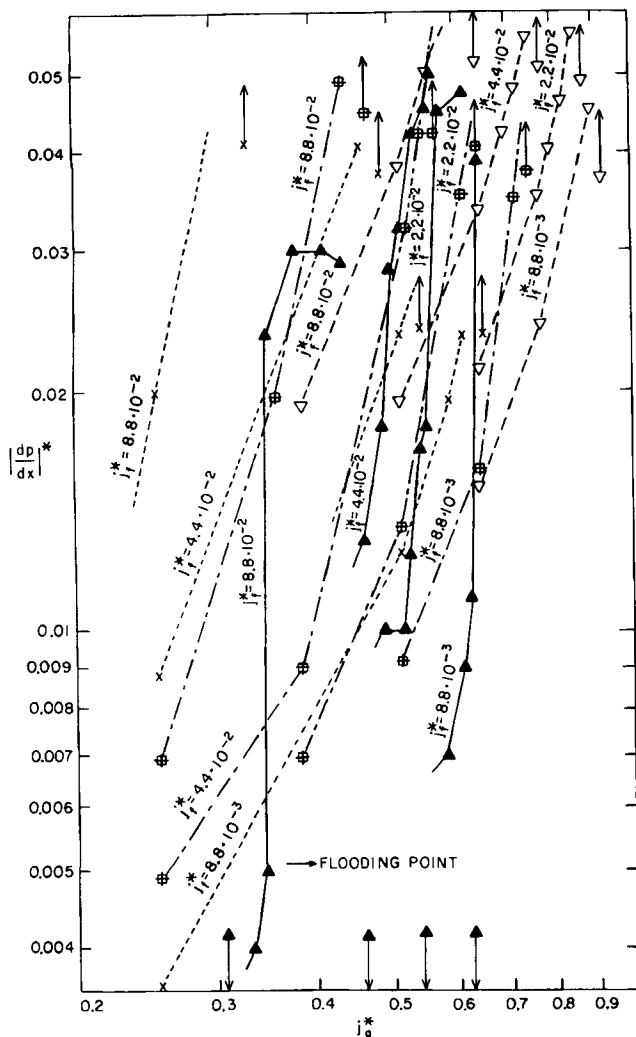


Figure 8. Pressure gradient prediction.

Conclusions

Most of the correlations for interfacial shear and entrainment have been developed from cocurrent data. The Bharathan-Wallis and Dukler correlations for the interfacial shear coefficient are two correlations available which have been developed from countercurrent data. It is shown here that except for the Bharathan-Wallis correlation, most of the correlations do not provide good agreement with the data when applied to the countercurrent flows. The advance codes such as TRAC-PF1 and COBRA-TF generally predict flooding at lower gas flow rates than in the test. They either have higher interfacial shear or a large entrainment rate, or both.

There is a definite lack of data for countercurrent flows. The University of Houston countercurrent flow test is one of the few well-instrumented tests available. Based on comparison with this test, the modified Wallis correlation or Bharathan-Wallis correlation for the interfacial shear coefficient and the modified Ishii correlation for entrainment have been suggested. More countercurrent flow data are needed to make a more definitive recommendation.

Acknowledgment

The work reported in this paper was made possible due to the International Atomic Energy Agency (IAEA), Vienna, Research Fellowship to

N. Popov during his stay at Brookhaven National Laboratory. Also, the general support of the U. S. Nuclear Regulatory Commission is gratefully acknowledged. The authors also thank Ann C. Fort for typing, and P. Saha for his encouragement.

Notation

- A = cross-sectional area of the pipe, m^2
- C_1 = constant, Eq. 1
- C_2 = constant, Eq. 2
- C_S = constant, Eq. 23
- d = pipe diameter, m
- E = droplet entrainment, %
- f_i = friction coefficient
- g = acceleration due to gravity, m/s^2
- H = pipe length, m
- j_i = volumetric flux, m/s
- K_i = Kutateladze number
- L_{eq} = pipe distance needed for equilibrium
- m = constant, Eq. 1
- n = constant, Eq. 2
- N_μ = viscosity number
- p = pressure, N/m^2
- P_i = perimeter, m
- r = radius, m
- Re = Reynolds number
- S = mass source, kg/s
- V_{dj} = droplet drift velocity, m/s
- V_f = phase velocity, m/s
- x = axial distance in the direction of film flow, m
- W = mass flow rate, kg/s
- We = Weber number

Greek letters

- α_i = phasic void fraction
- α_c = phasic void fraction in core
- δ = film thickness, m
- $\Delta\rho = \rho_l - \rho_g$ = density difference, kg/m^3
- μ_i = phasic dynamic viscosity, kg/ms
- ρ_i = phasic density, kg/m^3
- σ = surface tension, N/m
- τ = shear stress, N/m^2
- ψ = relaxation function

Subscripts

- c = core mixture
- $crit$ = critical for entrainment inception
- d = droplet
- e = entrained
- eq = equilibrium
- f = film
- g = gas
- i = refers to phase, f, g, d
- l = interface
- l = liquid
- r = relative
- w = wall

Superscripts

- $*$ = dimensionless
- $'$ = per unit length
- $''$ = per unit area

Literature Cited

- Bharathan D., G. B. Wallis, and H. J. Richter, "Air-Water Countercurrent Annular Flow," EPRI Report NP-1165, RP 443-2 (1979).
- Chu, K. J., and A. E. Dukler, "Statistical Characteristics of Thin Wavy Films. III: Structure of the Large Waves and Their Resistance to Gas Flow," *AIChE J.*, **21**(3), 585 (1975).
- Chung, K. S., C. P. Liu, and C. L. Tien, "Flooding in Two-Phase Countercurrent Flows. II: Experimental Investigation," *Physico-Chemical Hydrodynamics*, **1**, 209 (1980).

- Dukler, A. E., and L. Smith, "Two-Phase Interactions in Countercurrent Flow: Studies on the Flooding Mechanism," NUREG/CR-0617, Nuclear Regulatory Commission Report (Jan., 1979).
- Dukler, A. E., "Two-Phase Interactions in Countercurrent Flow," University of Houston, Annual Report, Nov. 1978–Oct. 1979 (1980).
- Henstock, W. H., and T. J. Hanratty, "The Interfacial Drag and the Height of the Wall Layer in Annular Flows," *AIChE J.*, **22**(6), 990 (1976).
- Hewitt, G. F., and G. B. Wallis, "Flooding and Associated Phenomena in Falling Film Flow in a Tube," AERE-R4022, Atomic Energy Research Establishment, Harwell, England (1963).
- Imura, H., H. Kusuda, and S. Funatsu, "Flooding Velocity in a Countercurrent Annular Two-Phase Flow," *Chem. Eng. Sci.*, **32**, 78 (1977).
- Ishii, M., and M. A. Grolmes, "Inception Criteria for Droplet Entrainment in Two-Phase Concurrent Film Flow," *AIChE J.*, **21**(2), 308 (1975).
- Ishii, M., T. C. Chowla, and N. Zuber, "Constitutive Equations for Vapor Drift Velocity in Two-Phase Annular Flow," *AIChE J.*, **22**, 283 (1976).
- Ishii, M., "One-Dimensional Drift-Flux Model and Constitutive Equations for Relative Motion Between Phases in Various Two-Phase Flow Regimes," AN-77-47, Argonne National Laboratory Report (Oct. 1977).
- Ishii, M., and K. Mishima, "Correlation for Liquid Entrainment in Annular Two-Phase Flow of Low Viscous Fluid," ANL/RAS/LWR 81-2, Argonne National Laboratory Report (Mar., 1981).
- Kutateladze, S. S., "Elements of Hydrodynamics of Gas-Liquid Systems," *Fluid Mechanics, Soviet Res.*, 29 (1972).
- Liles, D. R., et al., "TRAC-PF1, An Advanced Best-Estimate Computer Program for Pressurized Water Reactor Analysis," Los Alamos Scientific Laboratory (1981).
- Maron, D. M., and A. E. Dukler, "New Concepts on the Mechanisms of Flooding and Flow Reversal Phenomena," *Letters Heat and Mass Trans.*, **8**, 453 (1981).
- Popov, N. K., and U. S. Rohatgi, "Analysis of Countercurrent Adiabatic Flow Limitation Phenomena in Vertical Pipes" Brookhaven National Laboratory Report, to be pub. (1985).
- Ransom, V. H., et al., "RELAP5/MOD1 Code Manual, I: "System Models and Numerical Methods," EG&G Idaho Inc. (Mar., 1982).
- Shearer, C. J., and J. F. Davidson, "The Investigation of a Standing Wave Due to Gas Blowing Upwards Over a Liquid Film; Its Relation to Flooding in Wetted-Wall Columns," *J. Fluid Mech.*, **22**, 321 (1965).
- Tattersson, F. D., J. C. Dallman, and T. J. Hanratty, "Drop Sizes in Annular Gas-Liquid Flows," *AIChE J.*, **23**(1), 68 (1977).
- Thurgood, M. J., et al., "COBRA-TF Equations and Constitutive Models," Battelle, Pacific Northwest Laboratory (June, 1981).
- Tien, C. L., K. S. Chung., and P. Liu, "Flooding in Two-Phase Countercurrent Flows. I: Analytical Modeling," *Physico-Chemical Hydrodynamics*, **1**, 195 (1980).
- Wallis, G. B., *One-Dimensional Two-Phase Flow*, McGraw-Hill, New York (1969).
- , "Annular Two-Phase Flow. 1: A Simple Theory," *J. Basic Eng.*, **59** (Mar., 1970).
- , "Annular Two-Phase Flow. 2: Additional Effects," *J. Basic Eng.*, **73** (Mar., 1970).

Manuscript received Mar. 28, 1984, and revision received May 17, 1985.